arXiv:1401.5564v1 [cond-mat.mes-hall] 22 Jan 2014

Equal-Interval Splitting of Quantum Tunneling in Single-Molecule Magnets with Identical Exchange Coupling

Yan-Rong Li, Rui-Yuan Liu, Hai-Qing Liu and Yun-Ping Wang
Beijing National Laboratory for Condensed Matter Physics, Institute of Physics, Chinese Academy of Sciences, Beijing 100190, People's Republic of China
(Dated: January 23, 2014)

The equal-interval splitting of quantum tunneling observed in simple-Ising-model systems of Ni_4 (3D) and Mn_3 (2D) single-molecule magnets (SMMs) is reported. The splitting is due to the identical exchange coupling in the SMMs, and is simply determined by the difference between the two numbers of the spin-down $n_\downarrow$ and spin-up $n_\uparrow$ molecules neighboring to the tunneling molecule. The splitting may be presented as $(n_\downarrow - n_\uparrow)JS/g\mu_0\mu_B$, and the number of the splittings follows $n+1$ where $n = n_\downarrow + n_\uparrow$ is the coordination number. Besides, since the quantum tunneling is heavily dependent on local spin environment, the manipulation of quantum tunneling may become feasible for this kind of system, which may shed new light on novel applications of SMMs.

PACS numbers: 75.45.+j, 75.50.Xx, 05.50.+q 75.30.Et

Single-molecule magnets (SMMs) have been used as model systems to study the interface between classical and quantum behaviors, and are considered to be the most promising systems for the applications in quantum computing, high-density information storage and magnetic refrigeration [1–5] due to the quantum tunneling of magnetization (QTM) observed in these systems [6–9]. Recent researches in the impact of intermolecular exchange couplings upon the QTM have focused on whether the exchange coupling may change the quantum tunneling in SMMs. SMM dimer system is reported to have different quantum behavior from that of the individual SMMs, due to the intermolecular exchange couplings between the two components [10, 11]. It is also reported that, in the SMM dimer with 3D network of exchange-couplings, the QTM is not suppressed [12]. In this letter, we demonstrate that, for the SMMs with identical exchange coupling(IEC), the quantum tunneling behavior is much simpler and the QTM might be conveniently manipulated by controlling of the magnetization.

In the following, we report a unique quantum tunneling effect observed in the single-molecule magnets of $[Ni(hmp)(CH_3CH_2OH)Cl]_4$ (hereafter Ni_4) [13, 14] and $[Mn_3O(Et\text{-}sao)_3(MeOH)_3(ClO_4)]$ (hereafter Mn_3) [15, 16]. Ni_4 SMM is a crystal with 3D network of exchange coupling, in which each molecule is coupled with four neighboring molecules by Cl···Cl contact (which contributes to the exchange coupling) forming a diamond-like lattice. Ni_4 crystal has S_4 symmetry, which ensure that the four exchange couplings between each molecule and its four neighboring molecules are identical throughout the crystal. Mn_3 SMM is a crystal with 2D network of exchange coupling, in which each molecule is coupled with three neighboring molecules by hydrogen bonds (which contributes to the exchange coupling) in ab plain, forming a honeycomb-like structure viewed down along the c-axis. Mn_3 crystal has C_3 symmetry, which ensure that the three exchange couplings between each molecule and its three neighboring molecules are identical throughout the crystal. We notice that both Ni_4 and Mn_3 SMMs are crystals with IEC and the model systems of simple Ising model [17]. We have observed the equal-interval splitting of quantum tunneling induced by IEC in these two systems by ac susceptibility and hysteresis loop measurements.

Considering the low blocking temperature, we studied quantum tunneling effects of Ni_4 SMM by ac susceptibility measurements, with a home-made compensation measurement setup [18]. Fig.1 has demonstrated the temperature dependence of the quantum tunneling behavior in Ni_4 SMM. Apparently, the peak at zero field disappears at 0.75K and 0.5K, which consists with the missing step at zero field in magnetization hysteresis loops at 40mK [13]. As a result of different orientations, the step positions are different from those mentioned in Ref[13]. We measured the quantum tunnelings at different orientations and found the resonant fields along the easy axis

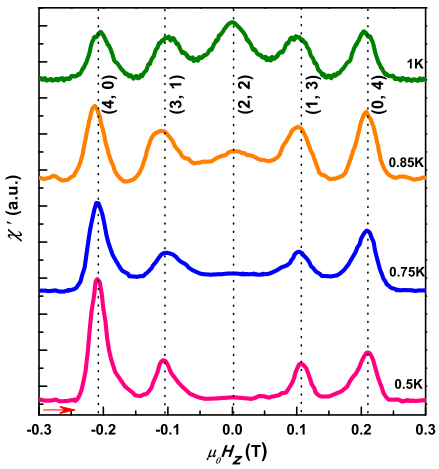

FIG. 1: (Color online). Field dependence of susceptibility χ' from -0.3T to 0.3T at different temperatures measured on Ni_4 single crystal, with the sweeping rate of 0.001T/s. The quantum tunneling peaks marked by black dotted lines origin from tunnelings between $|-4\rangle$ and $|4\rangle$ spin state, and the labeled number set in () besides each dotted line indicates the local spin environment $(n_\downarrow, n_\uparrow)$ of the tunneling molecules.

of the sample are −0.21T −0.11T, 0T, 0.11T, 0.21T as shown in Fig.1. It is seen that the tunneling peaks appear with equal interval. The shift of the tunneling peaks from higher to lower field with the increasing T is due to the enhancement of the effect of thermal activation upon tunneling [19, 20].

The higher blocking temperature allows us to study the hysteresis loops above 1.6K for Mn_3 SMM. Fig.2 shows the typical step-like hysteresis loops of Mn3 SMM at different temperatures. The blocking temperature estimated from ZFC (zero field cooling) and FC (field cooling) curves shown in the inset is around 3K. The sweep-rate-dependent magnetization curves at 1.6K are shown in Fig.3, with only a dM/dH curve at the sweeping rate of 0.0005T/s presented for simplicity. A series of quantum tunneling peaks with an equal interval of 0.36T are observed in the dM/dH curves, which is similar to those observed in Ni_4 SMM.

With IEC taken into account, the molecules are not isolated, and the spin Hamiltonian of each molecule may be presented as:

$$\hat{\mathcal{H}} = -D\hat{S}_z^2 + g\mu_0\mu_B\hat{S}_z H_z - \sum_{i=1}^{n} J\hat{S}_z\hat{S}_{iz}, \qquad (1)$$

where D is the axial anisotropy constant, n is coordination number, J is the exchange interaction constant, $\hat{S}_z$ and $\hat{S}_{iz}$ are the easy-axis spin operators of the molecule and its ith exchange-coupled neighboring molecule. For Ni_4, $S = 4$, $D = 0.86$K, $g = 2.12$ [13, 14]; while for Mn_3, $S = 6$, $D = 0.98$K, $g = 2.06$ [16].

In Ni_4 SMM, every Ni_4 molecule has four AFM exchange-coupled neighboring molecules, and hence for each molecule there are five different kinds of local spin environment (LSE), which may be labeled by $(n_\downarrow, n_\uparrow)$, where $n_\downarrow$ and $n_\uparrow$ represent the number of the neighboring molecules which occupy $S_z = -4$ (hereafter $|-4\rangle$) and $S_z = 4$ (hereafter $|4\rangle$) spin states respectively (The excited spin states are not considered here, because most of them are not populated at our measurement temperatures). At negative saturated field, all the molecules initially occupy $|-4\rangle$ in the same LSE $(4, 0)$ shown in Fig.4a (left). According to equation(1), $|-4\rangle$ and $|4\rangle$ spin states in the LSE $(4, 0)$ are degenerate when the field reaches $4JS/g\mu_0\mu_B$, therefore those molecules which occupy the $|-4\rangle$ spin state in the LSE (4, 0) (Fig.4a) have the same probability to undergo tunneling at $4JS/g\mu_0\mu_B$, leading to the resonant tunneling peaks at −0.21T as seen in Fig.1. Following this resonant quantum tunneling, some molecules will occupy $|4\rangle$ spin state, and the LSE of the molecules will not be identical any more. When the field reaches $2JS/g\mu_0\mu_B$ (corresponding to −0.11T as seen in Fig.1), the resonant tunneling takes place from $|-4\rangle$ to $|4\rangle$ spin state in the LSE (3, 1) (Fig.4b). As a matter of fact, at zero field the tunneling of the molecules in the LSE (2, 2) (Fig.4c) will change neither Zeeman energy nor the exchange interaction energy, which gives rise to the macroscopic quantum tunneling observed at zero field at relatively higher temperatures shown in Fig.1. Similarly, there are quantum tunnelings taking placing from $|-4\rangle$ to $|4\rangle$ spin state with the LSE (1, 3) at $-2JS/g\mu_0\mu_B$, and from $|-4\rangle$ to $|4\rangle$ spin state with the LSE (0, 4) at $-4JS/g\mu_0\mu_B$. The exchange interaction constant J is calculated to be −0.019K according to the splitting interval, which is close to the simulation value −0.02K obtained from the experimental AFM transition temperature of $T_N = 0.91$K [21]. At temperatures obviously below T_N, the spins of the molecules will be anti-parallel to its neighbors, i.e. the molecules are in the LSE (0, 4) and (4, 0) instead of the LSE (2, 2), which causes the missing of quantum tunneling at zero field at $T \leq 0.75$K

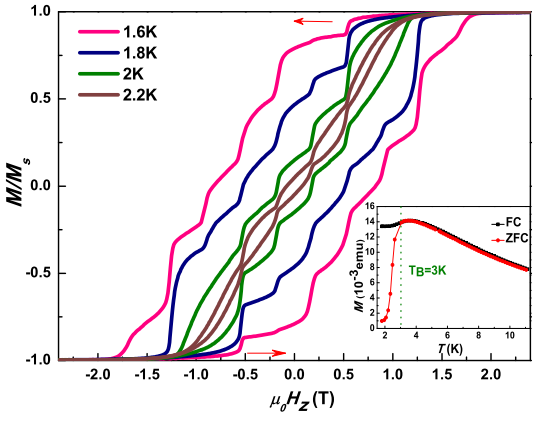

FIG. 2: (Color online). Magnetization (M/Ms) of Mn_3 single crystal versus applied magnetic field with the sweeping rate of 0.003T/s at different temperatures. The inset shows ZFC and FC curves.

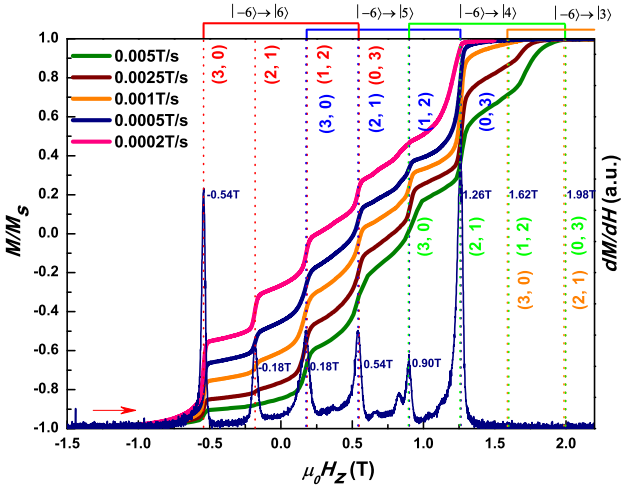

FIG. 3: (Color online). Sweep-rate-dependent magnetization (M/M_s) versus applied magnetic field $\mu_0 H_z$ (from −1.5T to 2.2T) at 1.6K measured on Mn_3 single crystal. dM/dH curve with sweeping rate of 0.0005T/s is given. The quantum tunneling peaks marked by the dotted lines of the same color belong to the same tunneling of $|m_i\rangle \rightarrow |m_f\rangle$, the labeled number set in () besides each dotted line indicates the local spin environment $(n_\downarrow, n_\uparrow)$ of the tunneling molecules.

as seen in Fig.1. However, in the vicinity of the transition temperature, some molecules are still in the LSE (2, 2) due to the thermal fluctuation, thus there is still an evidence of resonant quantum tunneling at 0.85K at zero field shown in Fig.1.

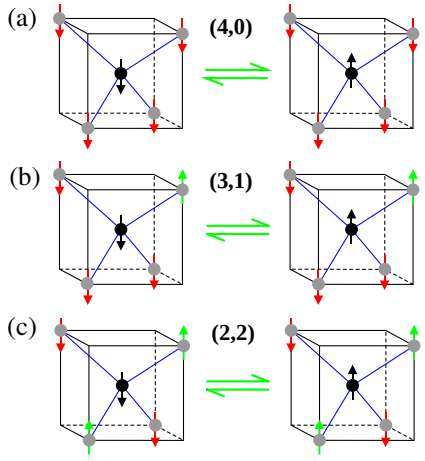

FIG. 4: (Color online). Sketch maps of three pairs of spin configurations with different LSE $(n_\downarrow, n_\uparrow)$ in Ni_4 SMM, in correspondence to the tunnelings occurring at -0.21T, -0.11T and 0T in Fig.1, respectively. Other equivalent spin configurations are not listed here for simplicity. The tunneling molecule is marked in black with black arrow indicating its spin state, its four neighbors are marked in gray, with green and red arrows indicating spin-up and spin-down state respectively, the blue lines between molecules represents the exchange couplings.

Mn_3 SMM displays a finer quantum tunneling behavior than Ni_4 SMM. Every Mn_3 molecule has three AFM exchange-coupled neighboring molecules, and hence for each molecule there are four different kinds of local spin environment as shown in Fig.5, labeled as (3, 0), (2, 1), (1, 2), (0, 3) respectively, thus, there are quantum tunnelings occurring at $3JS/g\mu_0\mu_B$, $JS/g\mu_0\mu_B$, $-JS/g\mu_0\mu_B$, $-3JS/g\mu_0\mu_B$ from $|-6\rangle$ to $|6\rangle$ spin state, which is corresponding to the four tunneling peaks marked by the red dotted lines shown in Fig.3.

In both Mn_3 and Ni_4 SMMs, with the presence of IEC, the tunneling between two ground spin states of $|\pm S\rangle$ is splitted by equal-interval field of $2|J|S/g\mu_0\mu_B$. Generally, according to equation(1), the tunneling from $|-S\rangle$ to $|S-l\rangle$ is splitted by the same equal-interval field, and the splitted tunneling field may be simply expressed as

$$H_z = lD/g\mu_0\mu_B + (n_\downarrow - n_\uparrow)JS/g\mu_0\mu_B. \qquad (2)$$

The first term comes from the internal spin states in each molecule, and the second term is of the tunneling splitting induced by IEC. The splitting is simply determined by the difference between the two numbers of the spin-down($n_\downarrow$) and spin-up ($n_\uparrow$) molecules neighboring to the tunneling molecule. According to equation(2), the number of splittings equals the number of different kinds of ($n_\downarrow$, $n_\uparrow$) LSEs, and hence may be expressed as $\binom{n+1}{1} = n+1$ by combinatorics, where $n = n_\downarrow + n_\uparrow$.

According to equation(2), when $D > n|J|S$ and $|H_z| < (D - n|J|S)/g\mu_0\mu_B$, any quantum tunneling with $l \neq 0$ are not allowed; while according to equation(1), when the first excitation energy of a molecule $D(2S-1) \gg kT$, almost all molecules will occupy the two ground spin states of $|\pm S\rangle$. Therefore, under the above conditions, equation(1) may be simplified as

$$\hat{\mathcal{H}} = g\mu_0\mu_B\hat{S}_z H_z - \sum_{i=1}^{n} J\hat{S}_z\hat{S}_{iz}, \qquad (3)$$

which is just the Hamiltonian of simple Ising model [17]. For both Ni_4 and Mn_3, $D > n|J|S$, thus Ni_4 and Mn_3 SMMs are good model systems of simple Ising model at low temperature and low field, which are important for the studies of quantum tunneling behavior and related applications.

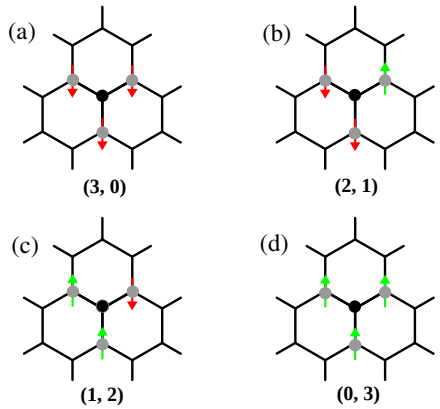

FIG. 5: (Color online). Sketch maps of four spin configurations with different LSE $(n_\downarrow, n_\uparrow)$ in Mn_3 SMM, other equivalent spin configurations are not listed here for simplicity. The tunneling molecule is marked in black, its three neighboring molecules are marked in grey, with green and red arrows indicating spin-up and spin-down state respectively. The black lines between molecules represent the exchange couplings.

Since the intermolecular exchange couplings are identical in the system, the magnitude $\mathcal{T}$ of a tunneling may be simply factorized into intermolecular contribution $N_{(n_\downarrow,n_\uparrow)}$ and intramolecular contribution $P_{|m_i\rangle\to|m_f\rangle}$,

$$\mathcal{T} = \alpha N_{(n_\downarrow,n_\uparrow)} P_{|m_i\rangle\to|m_f\rangle}, \qquad (4)$$

where $N_{(n_\downarrow,n_\uparrow)}$ is the number of molecules with the LSE $(n_\downarrow, n_\uparrow)$, $P_{|m_i\rangle\to|m_f\rangle}$ is the tunneling probability of the molecule from the spin state $|m_i\rangle$ to $|m_f\rangle$, and α is a constant. $N_{(n_\downarrow,n_\uparrow)}$ strongly depends on the magnetization M and may be easily modulated, while $P_{|m_i\rangle\to|m_f\rangle}$ is determined by the tunneling barrier between $|m_i\rangle$ and $|m_f\rangle$ inside molecules and is hardly to be controlled. Therefore, for SMMs-with-IEC, with the dependence of $\mathcal{T}$ on $N_{(n_\downarrow,n_\uparrow)}$, the manipulation of quantum tunneling should be rather simple.

The quantum tunnelings from the same initial states $|m_i\rangle$ to the same final states $|m_f\rangle$ but with different

LSEs are referred to as a tunneling set. The five tunneling peaks of Ni_4 SMM in Fig.1, belong to the same set of $|-4\rangle \rightarrow |4\rangle$ and has the same $P_{|m_i\rangle\rightarrow|m_f\rangle}$, thus the intensities of the five peaks is proportional to $N_{(n_\downarrow,n_\uparrow)}$, which means that $N_{(n_\downarrow,n_\uparrow)}$ may be monitored by macroscopic measurements of the tunneling peaks. For Mn_3 SMM, the AFM exchange coupling constant J is calculated to be $J = -0.041$K according to the field interval of the $|-6\rangle \rightarrow |6\rangle$ tunneling set(Fig.3). However the axial anisotropy constant $D = 0.98$K [16] of Mn_3 SMM happens to be close to $4|J|S$, which results in the overlap of two adjacent tunneling sets demonstrated by the overlapped dotted lines shown in Fig.3. The tunneling steps at 0.18T and 0.54T are the combinations of the tunnelings from $|-6\rangle$ to $|6\rangle$ spin state with the LSEs (1, 2) and (0, 3) (marked by red dotted lines) and quantum tunnelings from $|-6\rangle$ to $|5\rangle$ spin state with the LSEs (3, 0) and (2, 1) (marked by blue dotted lines) respectively. Similarly, all subsequent tunneling steps are combinations of quantum tunnelings in different tunneling sets with different local spin environments. It may be worth a mention that the tunnelings are expected to occur at 1.62T and 1.98T (marked by green and orange dotted lines) at lower temperatures as well, although not observed in these curves.

Of the overlapped tunnelings mentioned above, due to the dependence of tunneling on the local spin environment, the contribution of the individual tunneling changes as the field sweeping rate varies. For example, the tunneling step at 0.18T is the combination of tunneling from $|-6\rangle$ to $|6\rangle$ spin state with the LSE (1, 2) and tunneling from $|-6\rangle$ to $|5\rangle$ spin state with the LSE (3, 0), therefore the tunneling magnitude is determined by $N_{(3,0)}P_{|-6\rangle\rightarrow|5\rangle} + N_{(1,2)}P_{|-6\rangle\rightarrow|6\rangle}$, where $N_{(3,0)}$ and $N_{(1,2)}$ strongly depends on the magnetization M. As shown in Fig.3, for the tunneling at 0.18T, M/M_s is increasing with the decreasing of field sweeping rate, which suggests that $N_{(1,2)}$ is increasing while $N_{(3,0)}$ is decreasing, and hence the contribution of the tunneling from $|-6\rangle$ to $|6\rangle$ spin state with the LSE (1, 2) is taking the dominance from the contribution of the tunneling from $|-6\rangle$ to $|5\rangle$ spin state with the LSE (3, 0), eventually.

Due to the strong dependency of a tunneling on the $N_{(n_\downarrow,n_\uparrow)}$ based on equation(4), the subsequent quantum tunneling heavily depends on the the preceding quantum tunnelings in SMMs-with-IEC. As shown in Fig.3, tunneling at -0.54T (from $|-6\rangle$ to $|6\rangle$ spin state with the LSE (3, 0)) is inherited by tunneling at -0.18T (from $|-6\rangle$ to $|6\rangle$ spin state with the LSE (2, 1)), the tunnelings at -0.54T, -0.18T are further carried on by the next tunneling, and the process continues as the LSE changes. In fact, the history dependence is not prominent for Ni_4 SMM, due to that the measurements were performed at temperatures much higher than its blocking temperature, while thermal activated effect ruin the memory of history. Apparently, the subsequent quantum tunneling is more heavily dependent on the preceding quantum tunnelings in SMMs-with-IEC when the thermal activated effect is severely suppressed as the temperature drops adequately. This indicates a new way for manipulating quantum tunneling.

In summary, we performed detailed ac susceptibility and hysteresis loop measurements on Ni_4 and Mn_3 single crystals, respectively, and have observed the equal-interval splitting of quantum tunneling in both systems, the splitting of quantum tunneling is presented by $(n_\downarrow - n_\uparrow)JS/g\mu_0\mu_B$; and the number of splitting follows $n+1$, where $n = n_\downarrow + n_\uparrow$ is the coordination number. Since the splitting is induced by the IEC between the molecules, the rules should be universally applicable to all single-molecule magnets with IEC. Besides, it is demonstrated that, the manipulation of quantum tunneling may become feasible for this kind of system, which may shed new light on novel applications of SMMs.

We thank Prof. Dianlin Zhang, Lu Yu, and Li Lu for helpful discussions. We also thank Shaokui Su for experimental assistance. This work was supported by the National Key Basic Research Program of China (No.2011CB921702) and the Natural Science Foundation of China (No.11104331).

[1] M. N. Leuenberger and D. Loss, Nature **410**, 789 (2001).
[2] J. Tejada *et al.*, Nanotechnology **12**, 181 (2001).
[3] L. Bogani and W. Wernsdorfer, Nat. Mater. **7**, 179 (2008).
[4] J. Tejada, Polyhedron **20**, 1751 (2001).
[5] F. Torres *et al.*, Appl. Phys. lett. **77**, 3248 (2000).
[6] J. R. Friedman *et al.*, Phys. Rev. Lett. **76**, 3830 (1996).
[7] L. Thomas *et al.*, Nature **383**, 145(1996).
[8] C. Sangregorio *et al.*, Phys. Rev. Lett. **78**, 4645 (1997).
[9] K. L. Taft *et al.*, J. Am. Chem. Soc. **116**, 823 (1994).
[10] W. Wernsdorfer *et al.*, Nature **416**, 406 (2002).
[11] W. Wernsdorfer *et al.*, Phys. Rev. Lett. **89**, 197201 (2002).
[12] R. Tiron *et al.*, Phys. Rev .B **68**, 140407R (2003).
[13] E.-C. Yang *et al.*, Polyhedron **22**, 1727 (2003).
[14] E.-C. Yang *et al.*, Inorg. Chem. **45**, 529 (2006).
[15] R. Inglis *et al.*, Chem. Commun., 5924 (2008).
[16] R. Inglis *et al.*, Dalton Trans. 9157 (2009).
[17] H. A. Kramers and G. H. Wannier, Phys. Rev. **60**, 252 (1941)
[18] Y. R. Li *et al.*, Chin. Phys. Lett. **26**, 077504 (2009).
[19] L. Bokacheva, A. D. Kent, and M. A. Walters, Phys. Rev. Lett. **85**, 4803 (2000).
[20] J. J. Henderson *et al.*, Phys. Rev. Lett. **103**, 017202 (2009).
[21] J. W. Zuo *et al.*, Sci. China-Phys. Mech. Astron. **55**, 11 (2012).